

An equilibrated a posteriori error estimator for the interior penalty discontinuous Galerkin method

D. Braess, T. Fraunholz, Ronald H. W. Hoppe

Angaben zur Veröffentlichung / Publication details:

Braess, D., T. Fraunholz, and Ronald H. W. Hoppe. 2014. "An equilibrated a posteriori error estimator for the interior penalty discontinuous Galerkin method." *SIAM Journal on Numerical Analysis* 52 (4): 2121–36. <https://doi.org/10.1137/130916540>.



AN EQUILIBRATED A POSTERIORI ERROR ESTIMATOR FOR THE INTERIOR PENALTY DISCONTINUOUS GALERKIN METHOD*

D. BRAESS[†], T. FRAUNHOLZ[‡], AND R. H. W. HOPPE[§]

Abstract. Interior penalty discontinuous Galerkin (IPDG) methods for second order elliptic boundary value problems have been derived from a mixed variational formulation of the problem. Numerical flux functions across interelement boundaries play an important role in that theory. Residual type a posteriori error estimators for IPDG methods have been derived and analyzed by many authors including the convergence analysis of the resulting adaptive schemes. Typically, the effectivity indices deteriorate with increasing polynomial order of the IPDG methods. The situation is more favorable for a posteriori error estimators derived by means of the so-called hypercircle method. Equilibrated fluxes are obtained by using a mixed method and an extension operator for Brezzi–Douglas–Marini elements, and this can be done in the same way for all the discontinuous Galerkin methods that fit into a known unified framework. The hypercircle method immediately provides the reliability of the estimator, whereas its efficiency can be easily deduced from the efficiency of the residual operators. In contrast to the residual-type estimators, the new estimators do not contain unknown generic constants. Numerical results illustrate the performance of the suggested approach.

Key words. interior penalty discontinuous Galerkin method, a posteriori error estimation, equilibration

AMS subject classifications. 65N30, 65N15, 65N50

DOI. 10.1137/130916540

1. Introduction. Residual-type error estimates were the first estimates that have been studied in the a posteriori error analysis of discontinuous Galerkin (DG) elements; see, e.g., [6, 20, 21, 22, 25]. They are more involved than the analogous ones for conforming elements.

During the past decade, the hypercircle method also known as the Prager–Synge theorem and the two-energies principle (cf. [7, section III.9], [9, 10]) and the method of equilibrated fluxes (cf. [1, 2, 3, 4, 13, 14, 15, 16, 17, 18, 23, 24]) have attracted a lot of interest. The advantage is that the error bounds do not contain (unknown) generic constants. In this paper, we present a unified construction for all DG methods which are included in the general theory by Arnold et al. [5]. They present a mixed variational approach that is equivalent to the primal variational formulation. The specified numerical fluxes across the interelement boundaries are crucial in our construction. As an example, we consider the interior penalty discontinuous Galerkin (IPDG) method.

*Received by the editors April 11, 2013; accepted for publication (in revised form) May 28, 2014; published electronically August 19, 2014.

<http://www.siam.org/journals/sinum/52-4/91654.html>

[†]Faculty of Mathematics, Ruhr-University, D-44780 Bochum, Germany (Dietrich.Braess@rub.de).

[‡]Institut für Mathematik, Universität of Augsburg, D-86159 Augsburg, Germany (thomas.fraunholz@math.uni-augsburg.de). This author was supported by the DFG within the Priority Program SPP 1506.

[§]Department of Mathematics, University of Houston, Houston, TX 77204-3008 and Institut für Mathematik, Universität of Augsburg, D-86159 Augsburg, Germany (rohop@math.uh.edu, hoppe@math.uni-augsburg.de). This author was supported by NSF grants DMS-1115658, DMS-1216857, by the DFG within the Priority Program SPP 1506, by the BMBF within the Collaborative Research Projects “FROPT” and “MeFreSim,” and by the ESF within the Research Networking Programme “OPTPDE.”

The main task in the application of the hypercircle method is the construction of an equilibrated flux. Here it is achieved by the use of an extension operator for Brezzi–Douglas–Marini (BDM) elements in a postprocessing step. Thus it is similar to the construction in [13, 15, 18, 23] where instead Raviart–Thomas elements and mostly local Neumann problems have been used. In contrast to the cited papers we show that the hypercircle method and our construction apply to all DG methods listed in [5] and all polynomial degrees. Moreover, it simplifies the a posteriori analysis.

In fact, it readily provides the reliability of the estimator, whereas its efficiency can be derived from the efficiency of the residual operators. Our numerical calculations also show that the efficiency of the estimator does not deteriorate with increasing degree k of the polynomials in the DG finite element space, whereas the efficiency of residual estimates decreases linearly with the degree; cf. [9].

The consideration of the efficiency shows that the estimates share a property with the estimates of other nonconforming methods [2, 8]. The main contributions reflect the nonconformity, and there is no term referring to the element residual $\Delta u_h + f$ when we consider the discretization of problem (2.1).

Numerical results for two selected benchmark problems illustrate the performance of the estimator and confirm the theoretical findings.

Throughout this paper we will use standard notation from Lebesgue and Sobolev space theory [7]. In particular, for a bounded domain $\Omega \subset \mathbb{R}^2$ we denote by $(\cdot, \cdot)_{0,\Omega}$ and $\|\cdot\|_{0,\Omega}$ the inner product and the associated norm on the Hilbert space $L^2(\Omega)$. We further refer to $H^k(\Omega)$, $k \in \mathbb{N}$, as the Sobolev space with norm $\|\cdot\|_{k,\Omega}$ and seminorm $|\cdot|_{k,\Omega}$, whereas $H_0^k(\Omega)$ stands for the closure of $C_0^\infty(\Omega)$ with respect to the topology induced by $\|\cdot\|_{k,\Omega}$. Moreover, $H(\text{div}, \Omega)$ denotes the Hilbert space of vector fields $\in L^2(\Omega)^2$ such that $\text{div} \in L^2(\Omega)$ equipped with the graph norm.

2. Interior penalty discontinuous Galerkin method. For convenience, we consider the Poisson equation

$$(2.1) \quad \begin{aligned} -\Delta u &= f && \text{in } \Omega, \\ u &= 0 && \text{on } \Gamma, \end{aligned}$$

in a polygonal domain $\Omega \subset \mathbb{R}^2$ with homogeneous Dirichlet boundary conditions on $\Gamma = \partial\Omega$. The extension to more general second order elliptic differential operators and boundary conditions can be accommodated.

Let $\mathcal{T}_h(\Omega)$ be a simplicial triangulation of the computational domain Ω . Given $D \subset \bar{\Omega}$, we denote by $\mathcal{N}_h(D)$ and $\mathcal{E}_h(D)$ the set of vertices and edges of $\mathcal{T}_h(\Omega)$ in D , and we refer to $P_k(D)$, $k \in \mathbb{N}$, as the set of polynomials of degree $\leq k$ on D . Moreover, h_K , $K \in \mathcal{T}_h(\Omega)$, and h_E , $E \in \mathcal{E}_h(\bar{\Omega})$, stand for the diameter of K and the length of E , respectively, and $h := \max(h_K \mid K \in \mathcal{T}_h(\Omega))$. We consider the finite element approximation with the DG spaces

$$(2.2a) \quad V_h := \{v_h \in L^2(\Omega) \mid v_h|_K \in P_k(K), K \in \mathcal{T}_h(\Omega)\},$$

$$(2.2b) \quad \mathbf{V}_h := \{ \mathbf{v}_h \in L^2(\Omega)^2 \mid \mathbf{v}_h|_K \in P_k(K)^2, K \in \mathcal{T}_h(\Omega)\}.$$

For $E \in \mathcal{E}_h(\Omega)$, $E = K_+ \cap K_-$, $K_\pm \in \mathcal{T}_h(\Omega)$, and $v_h \in V_h$, we denote the average and jump of v_h across E by $\{v_h\}_E$ and $[v_h]_E$, i.e.,

$$\{v_h\}_E := \frac{1}{2} (v_h|_{E \cap K_+} + v_h|_{E \cap K_-}), \quad [v_h]_E := v_h|_{E \cap K_+} - v_h|_{E \cap K_-},$$

whereas for $E \in \mathcal{E}_h(\Gamma)$ we set

$$\{v_h\}_E := v_h|_E, \quad [v_h]_E := v_h|_E.$$

We follow the general scheme of DG methods in the mixed formulation as in [5] rather than the equivalent primal variational formulations. The finite element approximation of the Poisson equation with homogeneous Dirichlet boundary conditions amounts to the computation of $(u_h, \mathbf{h}) \in V_h \times \mathbf{V}_h$ such that for all $(v, \mathbf{v}) \in V_h \times \mathbf{V}_h$

$$(2.3a) \quad \int_{K \in \mathcal{T}_h(\Omega)} \mathbf{h} \cdot \nabla v \, dx = - \int_{K \in \mathcal{T}_h(\Omega)} u_h \operatorname{div} \mathbf{v} \, dx + \sum_{K \in \mathcal{T}_h(\Omega)} u_K \boldsymbol{\kappa}_K \cdot \mathbf{v} \, ds,$$

$$(2.3b) \quad \int_{K \in \mathcal{T}_h(\Omega)} \mathbf{h} \cdot \operatorname{grad} v \, dx = \int_{K \in \mathcal{T}_h(\Omega)} f v \, dx + \sum_{K \in \mathcal{T}_h(\Omega)} \boldsymbol{\kappa}_K \cdot \mathbf{v} \, ds,$$

where $\boldsymbol{\kappa}_K$ stands for the exterior normal unit vector on ∂K .

The definition of the DG method is completed by a rule for computing u_K and the numerical fluxes $\boldsymbol{\kappa}_K$, and each DG method is characterized by the associated definition. In particular, the IPDG method is obtained by the specification

$$(2.4) \quad \begin{aligned} u_K|_E &:= \{u_h\}_E, \\ \boldsymbol{\kappa}_K|_E &:= \{\operatorname{grad} u_h\}_E - h_E^{-1} [u_h]_E \boldsymbol{\nu}_E, \end{aligned} \quad E \in \mathcal{E}_h(\overline{\Omega}),$$

where $h_E > 0$ is a penalty parameter, and $h_E = 2.5(k+1)^2$ is considered as a convenient choice [19]. Here and below, for $E \in \mathcal{E}_h(\Omega)$, $E = K_+ \cap K_-$, $K_\pm \in \mathcal{T}_h(\Omega)$, the unit normal vector $\boldsymbol{\nu}_E$ is defined such that its product with a jump $[\cdot]_E$ is independent of the orientation of E , i.e., $[u_h]_E = u_h|_{K_-} - u_h|_{K_+} + u_h|_{K_+} - u_h|_{K_-}$.

For completeness, we recall the connection of the primal variational formulation and the mixed method for IPDG. Choosing $\mathbf{h} = \nabla v$ in (2.3a), using the integration by parts formula

$$(2.5) \quad \int_{K \in \mathcal{T}_h(\Omega)} u_h \operatorname{div} \nabla v \, dx = - \int_{K \in \mathcal{T}_h(\Omega)} \nabla u_h \cdot \nabla v \, dx + \sum_{K \in \mathcal{T}_h(\Omega)} u_h \boldsymbol{\kappa}_K \cdot \nabla v \, ds,$$

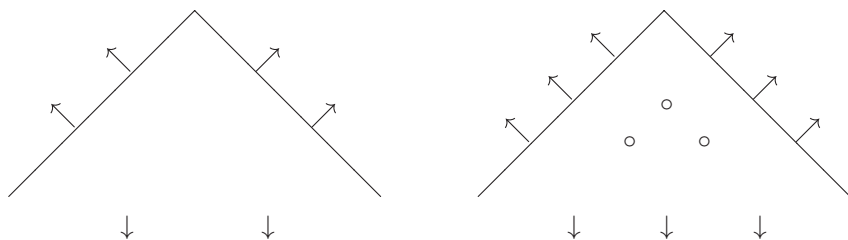
and eliminating \mathbf{h} from (2.3a), (2.3b) we obtain the primal variational formulation of the IPDG method: Find $u_h \in V_h$ such that for all $v \in V_h$

$$(2.6) \quad \begin{aligned} & \int_{K \in \mathcal{T}_h(\Omega)} \nabla u_h \cdot \nabla v \, dx - \sum_{E \in \mathcal{E}_h(\overline{\Omega})} \{ \nabla u_h \}_E \cdot [v]_E \boldsymbol{\nu}_E + [u_h]_E \cdot \{ \nabla v \}_E \boldsymbol{\nu}_E \, ds \\ & + \sum_{E \in \mathcal{E}_h(\overline{\Omega})} h_E^{-1} [u_h]_E [v]_E \, ds = \int_{K \in \mathcal{T}_h(\Omega)} f v \, dx. \end{aligned}$$

Conversely, if $u_h \in V_h$ solves (2.6), define $\mathbf{h} \in \mathbf{V}_h$ by

$$\int_{K \in \mathcal{T}_h(\Omega)} \mathbf{h} \cdot \nabla v \, dx = - \int_{K \in \mathcal{T}_h(\Omega)} u_h \operatorname{div} \mathbf{v} \, dx + \sum_{K \in \mathcal{T}_h(\Omega)} u_K \boldsymbol{\kappa}_K \cdot \mathbf{v} \, ds, \quad \mathbf{h} \in \mathbf{V}_h.$$

By setting $\mathbf{h} = \nabla v$, $v \in V_h$, and using the integration by parts formula (2.5) along with (2.6), it follows that the pair $(u_h, \mathbf{h}) \in V_h \times \mathbf{V}_h$ satisfies (2.3a), (2.3b). Hence, (2.3a), (2.3b), and (2.4) are equivalent to (2.6).

Fig. 1. DOFs of the BDM_1 element and of the BDM_2 element.

3. An interpolation by BDM elements. The numerical fluxes that live on the interelement boundaries will be extended to the elements by an interpolation. The finite element space for the fluxes is the BDM element, where $\mathbf{BDM}_k(K)$, $k \in \mathbb{N}$, is given by

$$(3.1) \quad \mathbf{BDM}_k(K) = P_k(K)^2, \quad \dim \mathbf{BDM}_k(K) = (k+1)(k+2).$$

We refer to $\frac{K}{i}$, $1 \leq i \leq 3$, as the barycentric coordinates of $K \in \mathcal{T}_h(\Omega)$ and denote by b_K the element bubble function $b_K := \frac{K}{1} \frac{K}{2} \frac{K}{3}$. By (3.41) in [11, p. 125] any $\mathbf{q}_K \in \mathbf{BDM}_k(K)$ is uniquely determined by the following degrees of freedom (DOF):

$$(3.2a) \quad \int_E \mathbf{q}_K \cdot \frac{K}{i} p_K ds, \quad p_K \in P_k(E), \quad E \in \mathcal{E}_h(K),$$

$$(3.2b) \quad \int_K \mathbf{q}_K \cdot \text{grad } p_{k-1} dx, \quad p_{k-1} \in P_{k-1}(K),$$

$$(3.2c) \quad \int_K \mathbf{q}_K \cdot \text{curl}(b_K p_{k-2}) dx, \quad p_{k-2} \in P_{k-2}(K).$$

A standard scaling argument yields a bound of the L^2 norm when a BDM element is interpolated with these data.

Lemma 3.1. *There exists a constant c that depends only on k and the shape regularity of \mathcal{T}_h such that for each $\mathbf{q}_K \in \mathbf{BDM}_k(K)$*

$$\begin{aligned} \int_K |\mathbf{q}_K(x)|^2 dx &\leq c \, h_K \int_K (\mathbf{q}_K \cdot \frac{K}{i})^2 ds \\ &\quad + h_K^2 \max_K (\mathbf{q}_K \cdot \text{grad } p)^2 dx; \quad p \in P_{k-1}, \quad \max_{x \in K} |p(x)| \leq 1 \\ &\quad + h_K^2 \max_K (\mathbf{q}_K \cdot \text{curl}(b_K p))^2 dx; \quad p \in P_{k-2}, \quad \max_{x \in K} |p(x)| \leq 1. \end{aligned}$$

Remark 3.2. For $k = 1$, $\mathbf{q}_K \in \mathbf{BDM}_1(K)$ is uniquely determined by the DOF on K ; cf. Figure 1.

Remark 3.3. A BDM element may be specified by $\text{div } \mathbf{q}_K$ instead of (3.2b). Therefore, the bound in Lemma 3.1 can be replaced by

$$\begin{aligned} \int_K |\mathbf{q}_K(x)|^2 dx &\leq c \, h_K \int_K (\mathbf{q}_K \cdot \frac{K}{i})^2 ds + h_K^2 \int_K (\text{div } \mathbf{q}_K)^2 dx \\ &\quad + h_K^2 \max_K (\mathbf{q}_K \cdot \text{curl}(b_K p))^2 dx; \quad p \in P_{k-2}, \quad \max_{x \in K} |p(x)| \leq 1. \end{aligned}$$

Moreover, we will refer to the following lemma.

Lemma 3.4. *There exists a constant c that depends only on k and the shape regularity of \mathcal{T}_h such that for each $\mathbf{q}_K \in \mathbf{BDM}_k(K)$*

$$\|\mathbf{q}_K \cdot \boldsymbol{\kappa}\|_{0,K} \leq ch_K^{-1/2} \|\mathbf{q}_K\|_{0,K}.$$

This inequality follows from the fact that

$$(3.3) \quad \inf_{\|\mathbf{q}_K \cdot \boldsymbol{\kappa}\|_{0,K}=1} \|\mathbf{q}_K\|_{0,K} > 0.$$

The constant c depends on the degree k , since (3.3) is not true, if we take the infimum over all H^1 functions.

4. Application of the hypercircle method to nonconforming finite elements. The starting point is the theorem of Prager and Synge [7, 27] that is also called the two-energies principle. We restrict ourselves to the Poisson equation; the generalization to other elliptic problems can be found in [7, Chap. III, section 9].

Theorem 4.1 (theorem of Prager and Synge, two-energies principle). *Let $\mathbf{f} \in H(\operatorname{div}, \Omega)$ and $v \in H_0^1(\Omega)$. Furthermore, let u be the solution of (2.1). If \mathbf{u} satisfies the equilibrium condition*

$$(4.1) \quad \operatorname{div} \mathbf{u} + f = 0,$$

then,

$$\|u - v\|_{1,\Omega}^2 + \|\operatorname{grad} u - \boldsymbol{\kappa}\|_{0,\Omega}^2 = \|\operatorname{grad} v - \boldsymbol{\kappa}\|_{0,\Omega}^2.$$

Supplement. Let $J(v) := \frac{1}{2} \|\operatorname{grad} v\|_{0,\Omega}^2 - \int_{\Omega} f v dx$ and $J^c(\boldsymbol{\kappa}) := \frac{1}{2} \|\boldsymbol{\kappa}\|_{0,\Omega}^2$ denote the (direct) energy and the complementary energy, respectively. If the assumptions above hold, then

$$\|u - v\|_{1,\Omega}^2 + \|\operatorname{grad} u - \boldsymbol{\kappa}\|_{0,\Omega}^2 = 2J(v) + 2J^c(\boldsymbol{\kappa}).$$

A proof is provided, e.g., in [7].

It is an advantage of the two-energies principle that the function v in Theorem 4.1 may be an auxiliary function which does not arise from a variational problem. The piecewise gradient of a finite element function v_h in the broken H^1 space will be denoted as $\operatorname{grad}_h v_h$. We have $\operatorname{grad}_h v_h \in L^2(\Omega)$.

Corollary 4.2. *Let u_h be the finite element solution of a nonconforming method in a broken H^1 space, e.g., a DG method. Assume that an auxiliary function $u_h^{\operatorname{conf}} \in H^1(\Omega)$ that satisfies the Dirichlet boundary condition, is obtained by postprocessing. Moreover, let $\mathbf{u}_h^{\operatorname{eq}} \in H(\operatorname{div}, \Omega)$ be a flow that satisfies the equilibrium condition (4.1). Then we have the estimate*

$$(4.2) \quad \begin{aligned} \|\operatorname{grad} u - \operatorname{grad}_h u_h\|_{0,\Omega} &\leq \|\operatorname{grad}_h u_h^{\operatorname{conf}} - \mathbf{u}_h^{\operatorname{eq}}\|_{0,\Omega} + \|\operatorname{grad}_h u_h - \operatorname{grad} u_h^{\operatorname{conf}}\|_{0,\Omega} \\ &\leq \|\operatorname{grad}_h u_h - \mathbf{u}_h^{\operatorname{eq}}\|_{0,\Omega} + 2\|\operatorname{grad}_h u_h - \operatorname{grad} u_h^{\operatorname{conf}}\|_{0,\Omega}. \end{aligned}$$

Indeed, the two-energies principle yields the following bound for the auxiliary function $u_h^{\operatorname{conf}}$:

$$\|\operatorname{grad} u - \operatorname{grad} u_h^{\operatorname{conf}}\|_{0,\Omega} \leq \|\operatorname{grad} u_h^{\operatorname{conf}} - \mathbf{u}_h^{\operatorname{eq}}\|_{0,\Omega}.$$

By applying the triangle inequality twice, we obtain (4.2).

The corollary was implicitly used in [2, 8].

In actual computations, we have frequently an additional term due to data oscillations. We only have the equilibration for an approximate function \bar{f} , i.e.,

$$\operatorname{div} \mathbf{v}_K + \bar{f} = 0$$

and $\int_K (\bar{f} - f) dx = 0$, $K \in \mathcal{T}_h(\Omega)$. The difference between the solutions of the Poisson equations for f and for \bar{f} will be estimated by the following lemma.

Lemma 4.3. *Let $\mathcal{T}_h(\Omega)$ be a triangulation of Ω , h_K denote the length of the longest side of $K \in \mathcal{T}_h(\Omega)$. If $g \in L^2(\Omega)$ satisfies*

$$(4.3) \quad \int_K g dx = 0, \quad K \in \mathcal{T}_h(\Omega),$$

then the solution of $-\Delta v = g$ in Ω with zero Dirichlet and/or Neumann boundary conditions satisfies

$$(4.4) \quad \|\nabla v\|_{0,\Omega} \leq \frac{1}{h_K^{1/2}} \left(\sum_{K \in \mathcal{T}_h(\Omega)} h_K^2 \|g\|_{0,K}^2 \right)^{1/2}.$$

A proof is given in [26]; see also [1]. Extra terms of the form (4.4) with $g := f - \bar{f}$ will cope with the data oscillation.

5. Equilibration. Let \bar{f} be the L^2 -projection of f onto piecewise polynomials of degree $k-1$, i.e.,

$$(5.1) \quad \int_K \bar{f} v dx = \int_K f v dx, \quad v \in P_{k-1}(K).$$

We construct a flux $\mathbf{v}_K \in \mathbf{BDM}_k(K)$ by the specifications

$$(5.2a) \quad \mathbf{v}_K|_K = \mathbf{v}_K,$$

$$(5.2b) \quad \int_K \mathbf{v}_K \cdot \operatorname{grad} p_{k-1} dx = \int_K \mathbf{h} \cdot \operatorname{grad} p_{k-1} dx, \quad p_{k-1} \in P_{k-1}(K),$$

$$(5.2c) \quad \int_K \mathbf{v}_K \cdot \operatorname{curl}(b_K p_{k-2}) dx = \int_K \mathbf{h} \cdot \operatorname{curl}(b_K p_{k-2}) dx, \quad p_{k-2} \in P_{k-2}(K).$$

The first equation corresponds to (3.2a) and shows that the flux is an extension of the numerical flux that is originally defined on the element boundaries. Now, it follows from (5.2b), Gauss' theorem, (5.1), and the DG finite element equation (2.3b) that

$$\begin{aligned} \operatorname{div} \mathbf{v}_K p_{k-1} dx &= - \int_K \mathbf{v}_K \cdot \operatorname{grad} p_{k-1} dx + \int_K \mathbf{v}_K \cdot \mathbf{n}_K p_{k-1} ds \\ &= - \int_K \mathbf{h} \cdot \operatorname{grad} p_{k-1} dx + \int_K \mathbf{v}_K \cdot \mathbf{n}_K p_{k-1} ds \\ (5.3) \quad &= - \int_K f p_{k-1} dx = - \int_K \bar{f} p_{k-1} dx. \end{aligned}$$

Since $\operatorname{div} \mathbf{v}_K$ and \bar{f} are contained in $P_{k-1}(K)$, we readily deduce from (5.3) that

$$\operatorname{div} \mathbf{v}_K + \bar{f} = 0.$$

By setting $\nu = 1$ in (5.1) we see that $f - \bar{f}$ satisfies the assumption (4.3), and the effect of the latter can be bounded by Lemma 4.3. Let $u_h \in H(\text{div}, \Omega)$ be defined by $u_h|_K = \kappa, K \in \mathcal{T}_h(\Omega)$, and we have obtained an equilibrated flux up to data oscillations.

The last specification (5.2c) aims at the minimization of the error bound with respect to the known quantities. This is one difference from the equilibration procedure by Ern and Vohralík [18] who used Raviart–Thomas elements.

Remark 5.1. If $k = 1$, due to Remark 3.2, κ is uniquely defined by (5.2a), that is by data of the numerical flux on the edges.

Note that up to now we have not used the specification (2.4) that distinguishes the interior penalty method IPDG from the other DG elements.

6. An approximation by conforming elements. Corollary 4.2 shows that we require an approximation of u_h by an H^1 function. We want to have a conforming element u_h^{conf} , and we will evaluate the norm

$$(6.1) \quad \|\text{grad } u_h^{\text{conf}} - \text{grad}_h u_h\|_{0,\Omega}$$

after computing the finite element approximations u_h and u_h^{conf} . We follow the construction in [21] that was used in connection with residual-based error estimates. The estimates of (6.1) in [21] will be useful in the verification of the efficiency and Theorem 6.1. We note that similar constructions and estimates are found in several papers.

Let \mathcal{N}^L be the set of Lagrangian nodal points for the elements in V_h . Let γ_i be the number of triangles that share the nodal point $x_i \in \mathcal{N}^L$. We have $\gamma_i = 1$ if x_i is contained in the interior of an element $K \in \mathcal{T}_h(\Omega)$ or if x_i is situated in the interior of an edge $E \in \mathcal{E}_h(\Gamma)$, while $\gamma_i > 1$ if $x_i \in \mathcal{N}^L \cap \mathcal{E}_h(\Omega)$. The multiplicity γ_i is bounded, since a minimal angle condition is assumed. The associated conforming element is now defined by its nodal values

$$(6.2) \quad u_h^{\text{conf}}(x_i) := \frac{1}{\gamma_i} \sum_{K \in \mathcal{T}_h(\Omega), x_i \in K} u_h|_K(x_i).$$

The following estimate is provided by Theorem 2.2 in [21]:

$$(6.3) \quad \|\text{grad } u_h^{\text{conf}} - \text{grad}_h u_h\|_{0,K}^2 \leq c \sum_{E \in \mathcal{E}_h(\bar{\Omega})} h_E^{-1} \| [u_h]_E \|^2_{0,E}.$$

The constant c depends only on the degree k of the finite elements and the shape regularity of the triangulation.

For sufficiently large penalty parameter, say $\gamma \geq \gamma_0$, the right-hand side of (6.3) can be bounded by Theorem 3.2(iv) in [22]:

$$(6.4) \quad \sum_{E \in \mathcal{E}_h(\bar{\Omega})} h_E^{-1} \| [u_h]_E \|^2_{0,E} \leq c \left(\|\text{grad } u - \text{grad}_h u_h\|_{0,\Omega}^2 + \sum_{K \in \mathcal{T}_h(\Omega)} h_K^2 \| f - \bar{f} \|_{0,K}^2 \right).$$

The last term on the right-hand side of (6.4) is added, since the analysis in [21] is done for zero data oscillation.

We note that β_1 can be larger than the minimal stability estimate for the IPDG method. For sharp bounds on the jump seminorm we refer to [2, 3]. From (6.4) we eventually obtain

$$(6.5) \quad \begin{aligned} & \| \text{grad } u_h^{\text{conf}} - \text{grad}_h u_h \|_{0,\Omega}^2 \\ & \leq c \quad \| \text{grad } u - \text{grad}_h u_h \|_{0,\Omega}^2 + \sum_{K \in \mathcal{T}_h(\Omega)} h_K^2 \| f - \bar{f} \|_{0,K}^2. \end{aligned}$$

This inequality will be used for the verification of the efficiency of the a posteriori error bound under consideration.

The inequality (6.5) is obtained from the efficiency of a residual a posteriori error estimate [21]. It gives rise to a comparison theorem for the solutions of two finite element methods in the spirit of the results in [8].

Theorem 6.1. *Let u_h^G be the solution of the Poisson equation by the conforming finite elements $V_h \cap H^1(\Omega)$ on the same triangulation. Then*

$$\| \text{grad}(u - u_h^G) \|_{0,\Omega} \leq c \quad \| \text{grad}_h(u - u_h) \|_{0,\Omega} + \sum_{K \in \mathcal{T}_h(\Omega)} h_K^2 \| f - \bar{f} \|_{0,K}^2. \quad 1/2$$

Proof. From the Galerkin orthogonality $(\text{grad}(u - u_h^G), \text{grad } v)_{0,\Omega} = 0$ for all $v \in V_h \cap H^1(\Omega)$ it follows that $\| \text{grad}(u - u_h^G) \|_{0,\Omega} \leq \| \text{grad}(u - u_h^{\text{conf}}) \|_{0,\Omega}$. Now we obtain from (6.5)

$$\begin{aligned} \| \text{grad}(u - u_h^G) \|_{0,\Omega} & \leq \| \text{grad}(u - u_h^{\text{conf}}) \|_{0,\Omega} \\ & \leq \| \text{grad}_h(u - u_h) \|_{0,\Omega} + \| \text{grad}_h(u_h - u_h^{\text{conf}}) \|_{0,\Omega} \\ & \leq \| \text{grad}_h(u - u_h) \|_{0,\Omega} \\ & \quad + c \quad \| \text{grad}_h(u - u_h) \|_{0,\Omega} + \sum_{K \in \mathcal{T}_h(\Omega)} h_K^2 \| f - \bar{f} \|_{0,K}^2, \end{aligned} \quad 1/2$$

and the proof is complete. \square

We note that the comparison theorem was established independently of the equilibration.

7. The error bound and its efficiency. Let $u_h \in H(\text{div}, \Omega)$ with $u_h|_K \in \mathbf{BDM}_k(K)$, $K \in \mathcal{T}_h(\Omega)$, be the equilibrated flux constructed according to (5.2) and let $u_h^{\text{conf}} \in V_h \cap H^1(\Omega)$ be defined by the averaging procedure from the previous section. Recalling Corollary 4.2 we introduce the estimator

$$(7.1) \quad \begin{aligned} \eta_{\text{hyp}} &:= \eta_{\text{hyp}}^{(1)} + \eta_{\text{hyp}}^{(2)}, \\ \eta_{\text{hyp}}^{(1)} &:= \sum_{K \in \mathcal{T}_h(\Omega)} \eta_K^{(1)}, \quad 1 \leq \eta_K^{(1)} \leq 2, \\ \eta_K^{(1)} &:= \| \text{grad}_h u_h - u_h \|_{0,K}, \quad \eta_K^{(2)} := 2 \| \text{grad}_h u_h - \text{grad } u_h^{\text{conf}} \|_{0,K}, \quad K \in \mathcal{T}_h(\Omega). \end{aligned}$$

By Corollary 4.2 and Lemma 4.3 we get the reliable a posteriori error estimate

$$(7.2) \quad \|\text{grad } u - \text{grad}_h u_h\|_{0,h} \leq_{\text{hyp}} + \frac{1}{h^{1/2}} \left(\sum_{K \in \mathcal{T}_h(\Omega)} h_K^2 \|f - \bar{f}\|_{0,K}^2 \right)^{1/2}.$$

From (6.5) it follows that the efficiency of the error bound (7.2) without the contribution of the data oscillation is guaranteed when we have appropriate bounds for $\|\text{grad}_h u_h - h\|_{0,\Omega}$. To this end, we will establish bounds for the terms in the triangle inequality $\|\text{grad}_h u_h - h\|_{0,\Omega} \leq \|\text{grad}_h u_h - h\|_{0,\Omega} + \|h - h\|_{0,\Omega}$.

First, (2.3a) and Gauss' theorem yield for $\mathbf{v} \in \mathbf{V}_h$

$$\begin{aligned} \int_K (h - \text{grad}_h u_h) \cdot \mathbf{v} \, dx &= \int_K h \cdot \mathbf{v} \, dx - \int_K \text{grad}_h u_h \cdot \mathbf{v} \, dx \\ &= - \int_K u_h \text{div } \mathbf{v} \, dx + \int_K u_{|K} \mathbf{v} \cdot \boldsymbol{\nu}_K \, ds \\ &\quad + \int_K u_h \text{div } \mathbf{v} \, dx - \int_K u_h \mathbf{v} \cdot \boldsymbol{\nu}_K \, ds \\ &= \int_K (u_{|K} - u_h) \mathbf{v} \cdot \boldsymbol{\nu}_K \, dx. \end{aligned}$$

It follows from the specification of the internal penalty method (2.4) that $\hat{u}_K - u_h = \frac{1}{2}[u_h]_E$ holds on $E \subset K$. We set $\mathbf{v} := h - \text{grad}_h u_h$, and a standard scaling argument yields

$$(7.3) \quad \|h - \text{grad}_h u_h\|_{0,K} \leq ch_K^{-1/2} \|[u_h]_K\|_{0,K}.$$

After summing over all elements we obtain with (6.4) the required bound for the left-hand side of (7.3),

$$\|h - \text{grad}_h u_h\|_{0,\Omega} \leq c \|\text{grad } u - \text{grad}_h u_h\|_{0,\Omega}^2 + \left(\sum_{K \in \mathcal{T}_h(\Omega)} h_K^2 \|f - \bar{f}\|_{0,K}^2 \right)^{1/2}.$$

Moreover, it follows from Lemma 3.4 and (7.3) that

$$(7.4) \quad \| (h - \text{grad}_h u_h) \cdot \boldsymbol{\nu}_K \|_{0,K} \leq ch_K^{-1} \|[u_h]_K\|_{0,K}.$$

Eventually we derive a bound for $h - h$. Lemma 3.1 together with (5.2b) and (5.2c) yields

$$\|h - h\|_{0,K} \leq ch_K^{1/2} \| (h - \text{grad}_h u_h) \cdot \boldsymbol{\nu}_K \|_{0,K}.$$

Recalling the specification (2.4) for the IPDG method, we obtain on $E \subset K$

$$\begin{aligned} h - h &= h - \text{grad}_h u_h + (\text{grad}_h u_h - h) \\ (7.5) \quad &= \frac{1}{2}[\text{grad}_h u_h]_E - h_E^{-1}[u_h]_E + (\text{grad}_h u_h - h). \end{aligned}$$

Let $E = K \cap K'$. Theorem 3.2(ii) in [22] asserts that

$$\begin{aligned} & \|[\text{grad}_h u_h]_E \cdot \nu\|_{0,E} \\ & \leq c h_K^{-1/2} \|\text{grad } u - \text{grad}_h u_h\|_{0,E} + h_K^2 \|f - \bar{f}\|_{0,K}^{1/2}, \end{aligned}$$

$K \in \mathcal{T}_h(\Omega)$

where $\mathcal{E}_h := \{K \in \mathcal{T}_h(\Omega) \mid E \in \mathcal{E}_h(K)\}$. The second term in (7.5) is already estimated in (6.4). The third term is reduced by (7.4) also to the second one, and we get

$$\begin{aligned} (7.6) \quad & \|\eta_h - \eta_h^{\text{conf}}\|_{0,\Omega} \\ & \leq c \sum_{K \in \mathcal{T}_h(\Omega)} \|\text{grad } u - \text{grad}_h u_h\|_{0,K}^2 + \sum_{K \in \mathcal{T}_h(\Omega)} h_K^2 \|f - \bar{f}\|_{0,K}^{1/2}. \end{aligned}$$

By collecting all terms we obtain the efficiency of the a posteriori error estimate deduced from Corollary 4.2.

Theorem 7.1. *Let u_h and η_h be the finite element solution of the IPDG method and the equilibrated flux, respectively. Further, assume that a conforming function u_h^{conf} has been constructed as described in section 6. There is a constant c that depends only on the degree k and the shape regularity of the triangulation such that*

$$\|\eta_h - \eta_h^{\text{conf}}\|_{0,\Omega} \leq c \|\text{grad } u - \text{grad}_h u_h\|_{0,\Omega} + \sum_{K \in \mathcal{T}_h(\Omega)} h_K^2 \|f - \bar{f}\|_{0,K}^{1/2}.$$

Remark 7.2. There is the natural question whether the efficiency of the bound (7.2) can also be obtained in a unified way. The contributions from the hypercircle method are bounded by the differences $\hat{u} - u_h$ and $\eta_h - \eta_h^{\text{conf}}$ on the interelement boundaries. Table 3.2 in [5] in turn shows that these differences can be expressed in terms of the jumps of u_h and $\eta_h \cdot \nabla u_h$ in many cases. The latter are found in the residual-based estimates; cf. [25]. If the efficiency of residual-based estimates is verified, we are done.

The treatment of $u_h - u_h^{\text{conf}}$ is independent of the origin of u_h .

8. Numerical results. In this section, we present a documentation of numerical results for two representative examples illustrating the performance of the suggested adaptive approach which consists of successive cycles of the steps

$$\text{SOLVE} \implies \text{ESTIMATE} \implies \text{MARK} \implies \text{REFINE}.$$

In the step SOLVE we compute the solution of the IPDG approximation (2.3), whereas the second step ESTIMATE is devoted to the computation of the local components $\eta_K^{(1)}$ and $\eta_K^{(2)}$ of the error estimator η_{hyp} (cf. (7.1)). We use the standard Dörfler marking in step MARK: Given some constant $0 < \theta \leq 1$, we choose a set $\mathcal{M} \subseteq \mathcal{T}_h(\Omega)$ of elements $K \in \mathcal{T}_h(\Omega)$ such that

$$(8.1) \quad \eta_{\text{hyp}} \leq \theta \left(\sum_{K \in \mathcal{M}} \eta_K^{(1)} + \sum_{K \in \mathcal{M}} \eta_K^{(2)} \right).$$

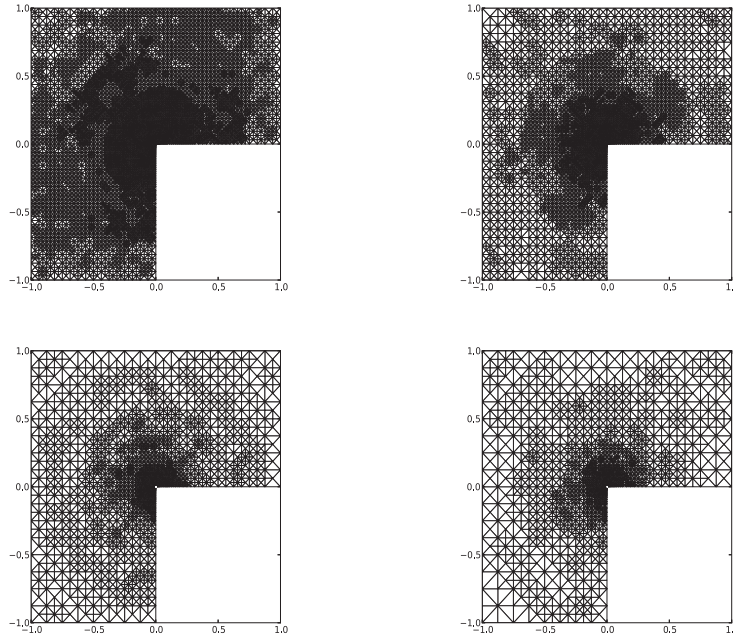


Fig. 2. Example 1: adaptively refined meshes for $k = 1$ (top left), $k = 2$ (top right), $k = 3$ (bottom left), and $k = 4$ (bottom right) after 9, resp., 12, 18, 23 adaptive cycles ($\theta = 0.3$ in the Dörfler marking).

The final step REFINE takes care of the practical realization of the refinement process which is based on the newest vertex bisection [12].

Example 1. We consider the Laplace equation with inhomogeneous Dirichlet boundary conditions

$$(8.2a) \quad -\Delta u = 0 \quad \text{in } \Omega,$$

$$(8.2b) \quad u = g \quad \text{on } \Omega$$

in the L-shaped domain $\Omega := (-1, +1)^2 \setminus ([0, +1] \times (-1, 0])$, where g in (8.2b) is chosen such that

$$u(r, \varphi) = r^{2/3} \sin(2\varphi/3)$$

is the exact solution (in polar coordinates). The solution exhibits a singularity at the origin.

For $\theta = 0.3$ in the Dörfler marking, Figure 2 displays the adaptively refined meshes for polynomial degrees $1 \leq k \leq 4$. As can be expected, the adaptive algorithm refines in the vicinity of the origin with coarser meshes for increasing polynomial degree k . For adaptive refinement ($\theta = 1$), $\theta = 0.7$, and $\theta = 0.3$, Figure 3 (left) shows the decrease of the global discretization error $\|\text{grad } u - \text{grad}_h u_h\|_{0,h}$ as a function of the total number of DOF on a logarithmic scale for polynomial degree $k = 1$ (top left) to $k = 4$ (bottom left). The negative slope is indicated for each curve. We see that for $\theta = 0.3$ the optimal convergence rates are approached asymptotically. Figure 3 (right) displays the associated effectivity indices (ratio of the a posteriori error estimator and the global discretization error). In contrast to standard residual type a posteriori

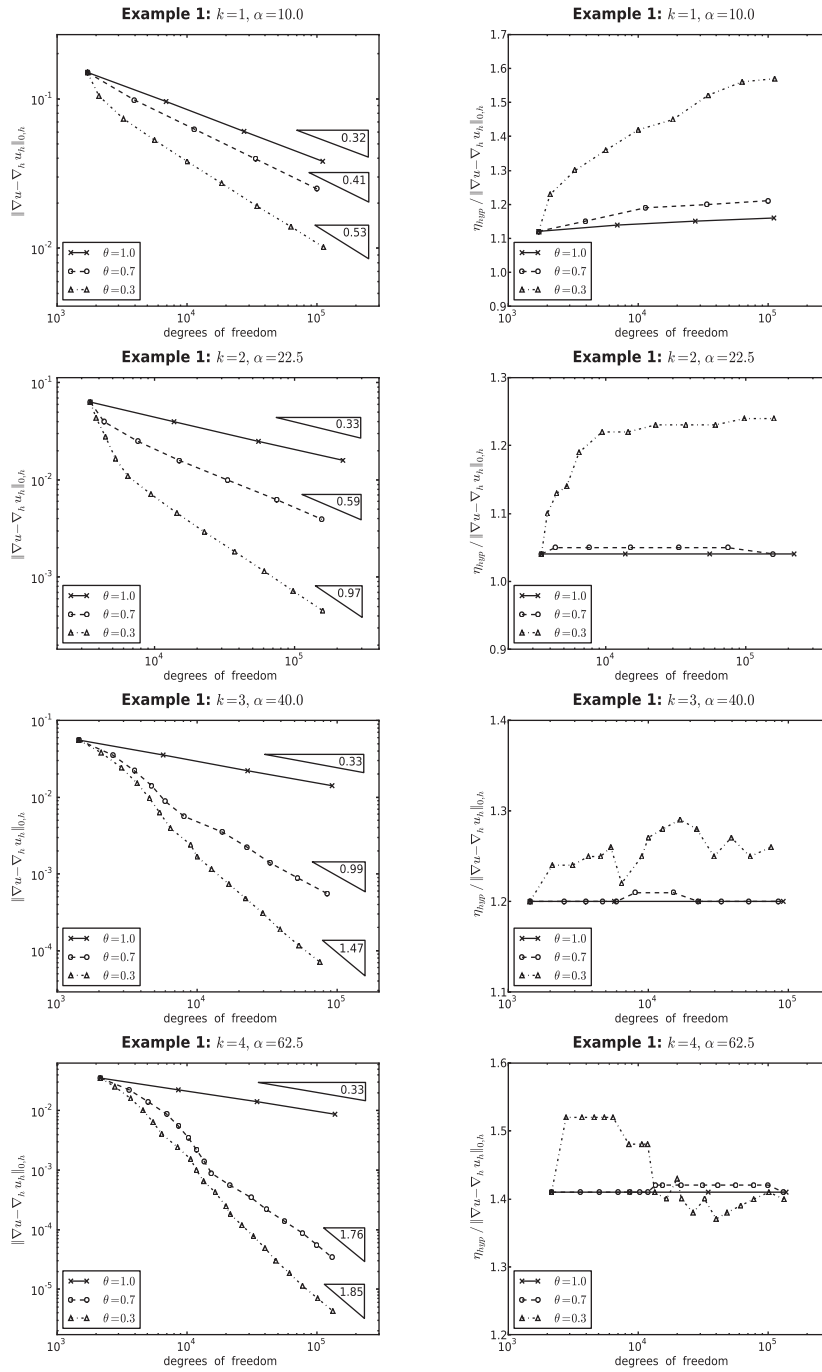


Fig. 3. Example 1: the discretization error $\|\text{grad } u - \text{grad}_h u_h\|_{0,h}$ as a function of the DOF on a logarithmic scale for various θ in the Dörfler marking (left) and the associated activity indices (right).

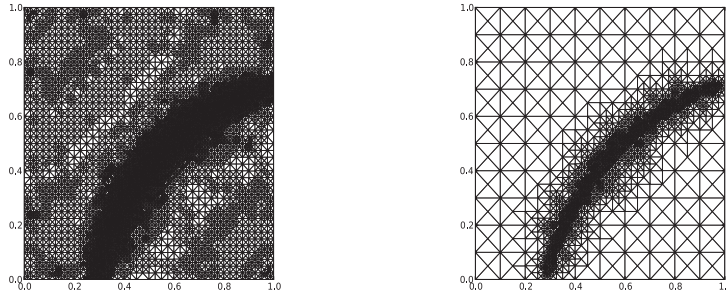


Fig. 4. Example 2: Adaptively refined meshes for $k = 1$ (left) and $k = 4$ (right) after 9 adaptive cycles ($\theta = 0.3$ in the Dörfler marking).

error estimators for IPDG approximations, the effectivity indices are slightly above 1 and do not significantly deteriorate with increasing polynomial degree k .

Example 2. We consider Poisson's equation with homogeneous Dirichlet boundary conditions

$$(8.3a) \quad -\Delta u = f \quad \text{in } \Omega,$$

$$(8.3b) \quad u = 0 \quad \text{on } \Omega$$

in the unit square $\Omega = (0, 1)^2$, where the right-hand side f in (8.3a) is chosen such that

$$u(x, y) = x(1-x)y(1-y) \arctan(60(r-1)), \quad r^2 := (x-5/4)^2 + (y+1/4)^2$$

is the exact solution. The solution exhibits an interior layer along a circular segment inside the computational domain.

Figure 4 shows the adaptively refined meshes for polynomial degree $k = 1$ and $k = 4$ in the case of $\theta = 0.3$ in the Dörfler marking, whereas for uniform refinement ($\theta = 1$), $\theta = 0.7$ and $\theta = 0.3$. Figure 5 displays the global discretization error as a function of the DOF on a logarithmic scale (left) and the associated effectivity indices (right). We see that both for $\theta = 0.7$ and $\theta = 0.3$ the optimal convergence rates are achieved asymptotically and that the effectivity indices even slightly improve with increasing polynomial degree k .

9. Concluding remarks. The design of the a posteriori error bound is the same for all discontinuous Galerkin methods. There is no generic constant, and the proof of the reliability is much easier than that for residual-based estimators. In essence, it is focused on the terms which measure the nonconformity.

The proof of the efficiency is very similar to the analysis of residual-based error estimates, but there is one term less. The typical term

$$h \|\Delta u_h + f\|_{0,\Omega}$$

that models the negative norm $\|\Delta u_h + f\|_{-1}$ is not present, since implicitly a left inverse of the divergence operator is involved. The left inverse is constructed by a local procedure.

We recall that the analysis is based on the mixed formulation in [5], and it is known (see [8]) that the efficiency of the estimator is related to the quality of the mixed finite element method; cf. the comparison (7.6).

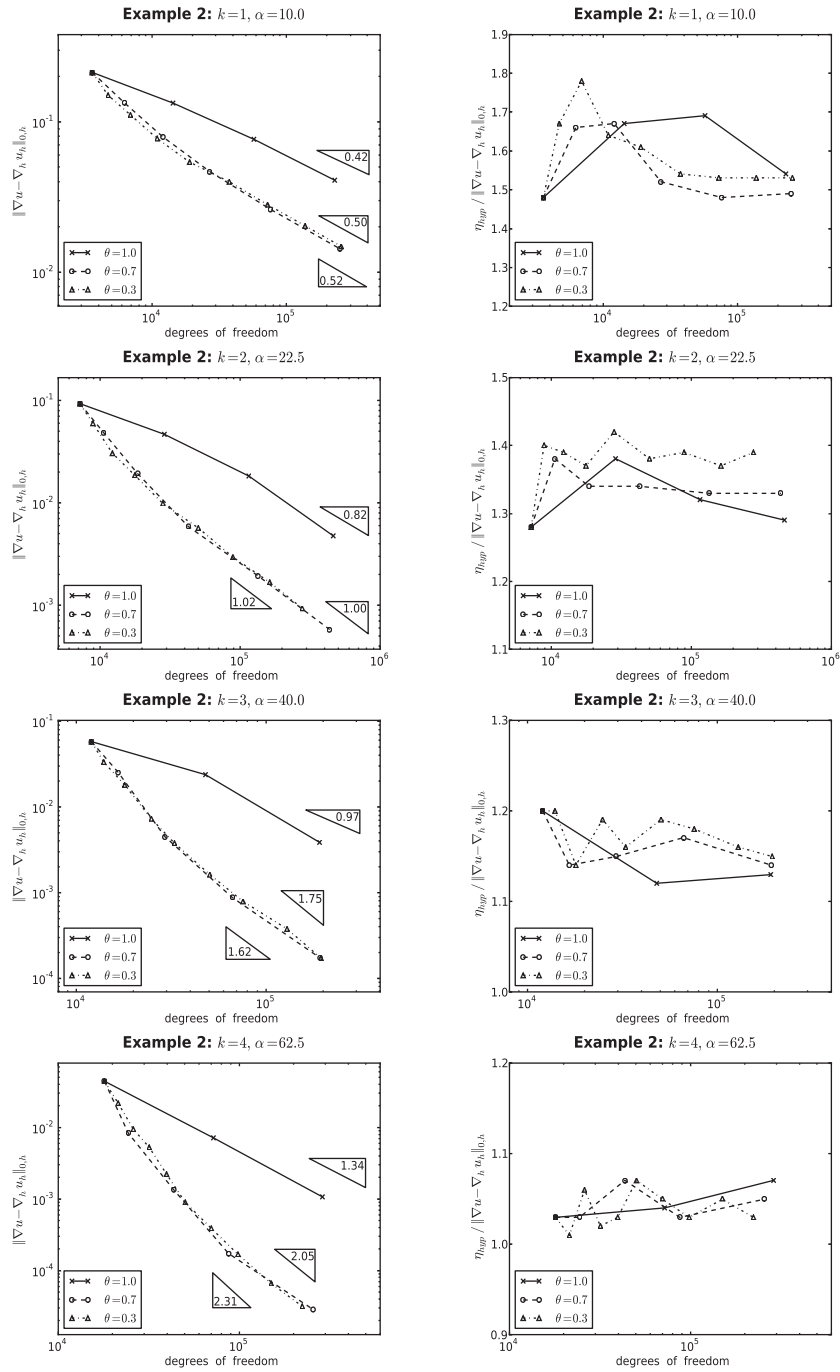


Fig. 5. Example 2: the discretization error $\|\text{grad } u - \text{grad}_h u_h\|_{0,h}$ as a function of the DOF on a logarithmic scale for various θ in the Dörfler marking (left) and the associated activity indices (right).

REFERENCES

- [1] M. Ainsworth, *A posteriori error estimation for discontinuous Galerkin finite element approximation*, SIAM J. Numer. Anal., 45 (2007), pp. 1777–1798.
- [2] M. Ainsworth, *A posteriori error estimation for lowest order Raviart Thomas mixed finite elements*, SIAM J. Sci. Comput., 30 (2008), pp. 189–204.
- [3] M. Ainsworth and R. Rankin, *Fully computable error bounds for discontinuous Galerkin finite element approximations on meshes with an arbitrary number of levels of hanging nodes*, SIAM J. Numer. Anal., 47 (2010), pp. 4112–4141.
- [4] M. Ainsworth and R. Rankin, *Constant free error bounds for non-uniform order discontinuous Galerkin finite element approximation on locally refined meshes with hanging nodes*, IMA J. Numer. Anal., 31 (2011), pp. 254–280.
- [5] D. N. Arnold, F. Brezzi, B. Cockburn, and L. D. Marini, *Unified analysis of discontinuous Galerkin methods for elliptic problems*, SIAM J. Numer. Anal., 39 (2002), pp. 1749–1779.
- [6] A. Bonito and R. H. Nochetto, *Quasi-optimal convergence rate of an adaptive discontinuous Galerkin method*, SIAM J. Numer. Anal., 48 (2010), pp. 734–771.
- [7] D. Braess, *Finite Elements: Theory, Fast Solvers and Applications in Solid Mechanics*, 3rd ed., Cambridge University Press, Cambridge, 2007.
- [8] D. Braess, *An a posteriori error estimate and a comparison theorem for the nonconforming P_1 element*, Calcolo, 46 (2009), pp. 149–156.
- [9] D. Braess, V. Pillwein, and J. Schöberl, *Equilibrated residual error estimates are p-robust*, Comput. Methods Applied Mech. Engrg., 198 (2009), pp. 1189–1197.
- [10] D. Braess and J. Schöberl, *Equilibrated residual error estimator for edge elements*, Math. Comp., 77 (2008), pp. 651–672.
- [11] F. Brezzi and M. Fortin, *Mixed and Hybrid Finite Element Methods*, Springer, Berlin, 1991.
- [12] J. M. Cascon, C. Kreuzer, R. H. Nochetto, and K. G. Siebert, *Quasi-optimal convergence rate for an adaptive finite element methods*, SIAM J. Numer. Anal., 46 (2008), pp. 2524–2550.
- [13] S. Cochez-Dhondt and S. Nicaise, *Equilibrated error estimators for discontinuous Galerkin methods*, Numer. Methods Partial Differential Equations, 24 (2008), pp. 1236–1252.
- [14] D. A. Di Pietro and A. Ern, *Mathematical Aspects of Discontinuous Galerkin Methods*, Springer, Berlin, 2012.
- [15] A. Ern, S. Nicaise, and M. Vohralík, *An accurate $H(\text{div})$ flux reconstruction for discontinuous Galerkin approximations of elliptic problems*, C. R. Acad. Sci. Paris Sér. I Math., 345 (2007), pp. 709–712.
- [16] A. Ern and A. F. Stephansen, *A posteriori energy-norm error estimates for advection-diffusion equations approximated by weighted interior penalty methods*, J. Comput. Math., 26 (2008), pp. 488–510.
- [17] A. Ern, A. F. Stephansen, and M. Vohralík, *Guaranteed and robust discontinuous Galerkin a posteriori error estimates for convection-diffusion-reaction problems*, J. Comput. Appl. Math., 234 (2010), pp. 114–130.
- [18] A. Ern and M. Vohralík, *Flux reconstruction and a posteriori error estimation for discontinuous Galerkin methods on general nonmatching grids*, C. R. Acad. Sci. Paris Sér. I Math., 347 (2009), pp. 4441–4444.
- [19] J. S. Hesthaven and T. Warburton, *Nodal Discontinuous Galerkin Methods: Algorithms, Analysis, and Applications*, Springer, Berlin, 2008.
- [20] R. H. W. Hoppe, G. Kanschat, and T. Warburton, *Convergence analysis of an adaptive interior penalty discontinuous Galerkin method*, SIAM J. Numer. Anal., 47 (2009), pp. 534–550.
- [21] O. A. Karakashian and F. Pascal, *A posteriori error estimates for a discontinuous Galerkin approximation of second-order elliptic problems*, SIAM J. Numer. Anal., 41 (2003), pp. 2374–2399.
- [22] O. A. Karakashian and F. Pascal, *Convergence of adaptive discontinuous Galerkin approximations of second-order elliptic problems*, SIAM J. Numer. Anal., 45 (2007), pp. 641–665.
- [23] K.-Y. Kim, *A posteriori error analysis for locally conservative mixed methods*, Math. Comp., 76 (2007), pp. 43–66.
- [24] R. Lazarov, S. Repin, and S. Tomar, *Functional a posteriori error estimates for discontinuous Galerkin approximations of elliptic problems*, Numer. Methods Partial Differential Equations, 25 (2009), pp. 952–971.

- [25] C. Lovadina and L. D. Marini, *A-posteriori error estimates for discontinuous Galerkin approximations of second order elliptic problems*, J. Sci. Comput., 40 (2009), pp. 340–359.
- [26] L. E. Payne and H. F. Weinberger, *An optimal Poincaré inequality for convex domains*, Arch. Ration. Mech. Anal., 5 (1960), pp. 286–292.
- [27] W. Prager and J. L. Synge, *Approximations in elasticity based on the concept of function spaces*, Quart. Appl. Math., 5 (1947), pp. 241–269.